Supplementary Information

Solution-based fabrication of a highly catalytically active 3D network constructed from 1D metal-organic framework-coated polymeric worm-like micelles

Junqi Yi, Haodong Li, Li Jiang, Kaka Zhang, Daoyong Chen*

The State Key Laboratory of Molecular Engineering of Polymers, department of Macromolecular Science, Fudan University, Handan Road 220, Shanghai 200433, P. R. China

S1: Characterization

Field-Emission Scanning Electron Microscope (FESEM) images were taken on un-coated samples using Zeiss Ultra 55 Field-Emission SEM with an accelerating voltage of 2 KV. Transmission Electron Microscope (TEM) images were taken by FEI Tecnai G2 20 TWIN at 200 KV and by Philips CM120 at 80 kV. Powder X-ray diffraction (PXRD) dates were collected with PANalytical X'pert PRO using Cu Kα radiation. Thermogravimetric Analysis was carried out on PE Pyris 1 TGA. Typically, about 2 mg of sample was tested under Air flow and heated at a rate of 40 °C/min from 50 °C to 800 °C. Nitrogen sorption isotherms were measured at 77 K using Micromeritics ASAP 2020. Before measurements, samples were degased for 10h at 120 °C. Selected area electron diffraction (SAED) and High-Resolution Transmission Electron Microscope (HRTEM) were performed on JEM-2100F at 200 KV. Zeta. Mercury intrusion porosimetry were measured using Micromeritics' AutoPore IV Porosimeter.

S2: Synthesis of polymeric worm-like micelles (PWs)

The PWs were prepared through self-assembly of DNA and PEG_{113}-*b*-$P4VP_{118}$ micelles according to our previously reported methods.[1] In order to stabilize the fiber-like structure of PWs, 1,4-dibromobutane was added to crosslink the P4VP core. Typically, for the 1000 mL of the as-synthesis mixture of PW with a concentration of 2 mg/mL, 81 μL (crosslinking degree: 10%) or 0.85 mL (crosslinking degree: 100%) of 1,4-dibromobutane was added to crosslink the P4VP core. The mixture was then stirred for another 2 days before use. The synthesized crosslinked PWs were collected via centrifugation at 12,000 rpm, washed with water twice and freeze dried.

Through this method, a large amount of pure PWs with a uniform width of 28 nm (Figure S1) and a crosslinked P4VP core was obtained, which is precondition for the large scale preparation of the composite nanowires; such a large amount (gram quantities) of pure PWs capable of collection and re-dispersion is difficult for conventional methods to prepare. The PWs are stable, as indicated by no changes being observed in the structure or morphology of the PWs during dispersion in common solvents or during composite preparation. Moreover, the PWs were well-dispersed even at a relatively high concentration (e.g., 2 mg/mL) in water or methanol for 1 year.

The PWs with Au nanoparticles in their core were prepared as follows. First, an aqueous solution of $HAuCl_4$ (10 mg/mL, 5 mL) and an aqueous solution of Na_2CO_3 (20 mg/mL, 5 mL) were added to the synthesized 10% crosslinked PW aqueous solution (2 mg/mL, 5 mL), and the resulting mixture was stirred at room temperature for 1 h. Excess aqueous solution of $NaBH_4$ was added to yield Au nanoparticles. Silicified PWs were fabricated through the following steps. First, the pH of the 10% crosslinked PW aqueous solution (2 mg/ml, 10 mL) was adjusted to 5 using hydrochloric acid. TEOS (40 mg) was subsequently added, and the solution was stirred at room temperature for 48 h.

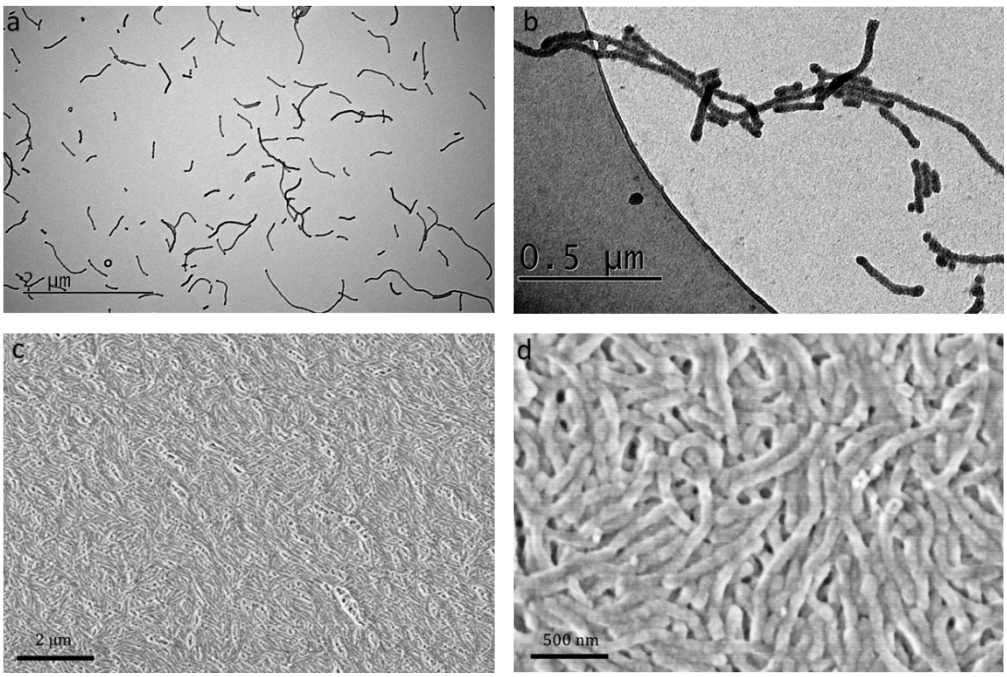

Figure S1. a) TEM image of the PWs with a PEG shell and a crosslinked P4VP core (crosslinking degree: 10%). Without being stained, the PEG shell is invisible and the cylindrical crosslinked P4VP cores are visible. b) PWs with Au nanoparticles loaded by the P4VP core. c, d) FESEM images of silicified PWs prepared by hydrolysis of tetramethoxysilane within the PWs. PWs were polymers that can easily become a film or have an ambiguous contour profile when cast onto substrates that can be modified by silicification.

Table S1. Statistic average length of PWs based on TEM image

The length of PW(nm)												
409.8	172.4	1319.9	550.8	1222.3	476.0	2768.4	664.2	1091.1	512.2	1072.6	531.7	975.4
627.6	399.5	178.5	252.4	196.7	895.4	611.7	382.5	583.2	519.1	362.3	495.9	679.5
1239.1	1817.6	295.2	104.6	1874.4	1151.6	480.7	642.9	958.8	305.9	436.2	715.8	342.4
83.1	470.7	294.2	3044.4	1181.3	827.9	529.7	1082.0	830.3	595.3	160.5	136.0	212.6
128.4	500.8	1369.7	582.1	681.9	1271.8	840.5	269.3	238.8	230.2	281.7	89.2	
average length (L): 691 nm												

S3: Synthesis of 3D network, individual composite nanowire and pure ZIF-8

For preparing the 3D network, 50 mL of a methanol solution of zinc nitrate hexahydrate (Zn2+) at 250 mM (74.4 mg/mL) and 100 mL of a methanol solution of 2-methylimidazole (Hmim) at 250 mM (20.5 mg/mL) were added successively to 850 mL of a PW suspension at a concentration of 0.094 mg/mL. In the final mixture, the concentrations of the PWs, Zn2+ and Hmim were 0.08 mg/mL, 3.72 mg/mL and 2.05 mg/mL, respectively. The mixture was then briefly shaken and subsequently incubated at room temperature for 24 h without being stirred. For preparing gram quantities of product, we repeated the above experiment four times and the yield was 1.86 g in total. Individual composite nanowires were prepared by reducing the concentration of PWs to 0.04 mg/mL in the reaction mixture. For the preparation of pure ZIF-8 nano- and micro-crystals, the concentration of Zn2+ and Hmim were 3.72 mg/mL, 2.05 mg/mL (nanocrystal) and 18.6 mg/mL, 10.3 mg/mL (microcrystal), respectively. All products were collected by centrifugation at 5000 rpm, washed with methanol three times, dried under vacuum overnight and activated at 120 °C under vacuum for 10 h.

S4: FESEM and TEM images of the 3D network

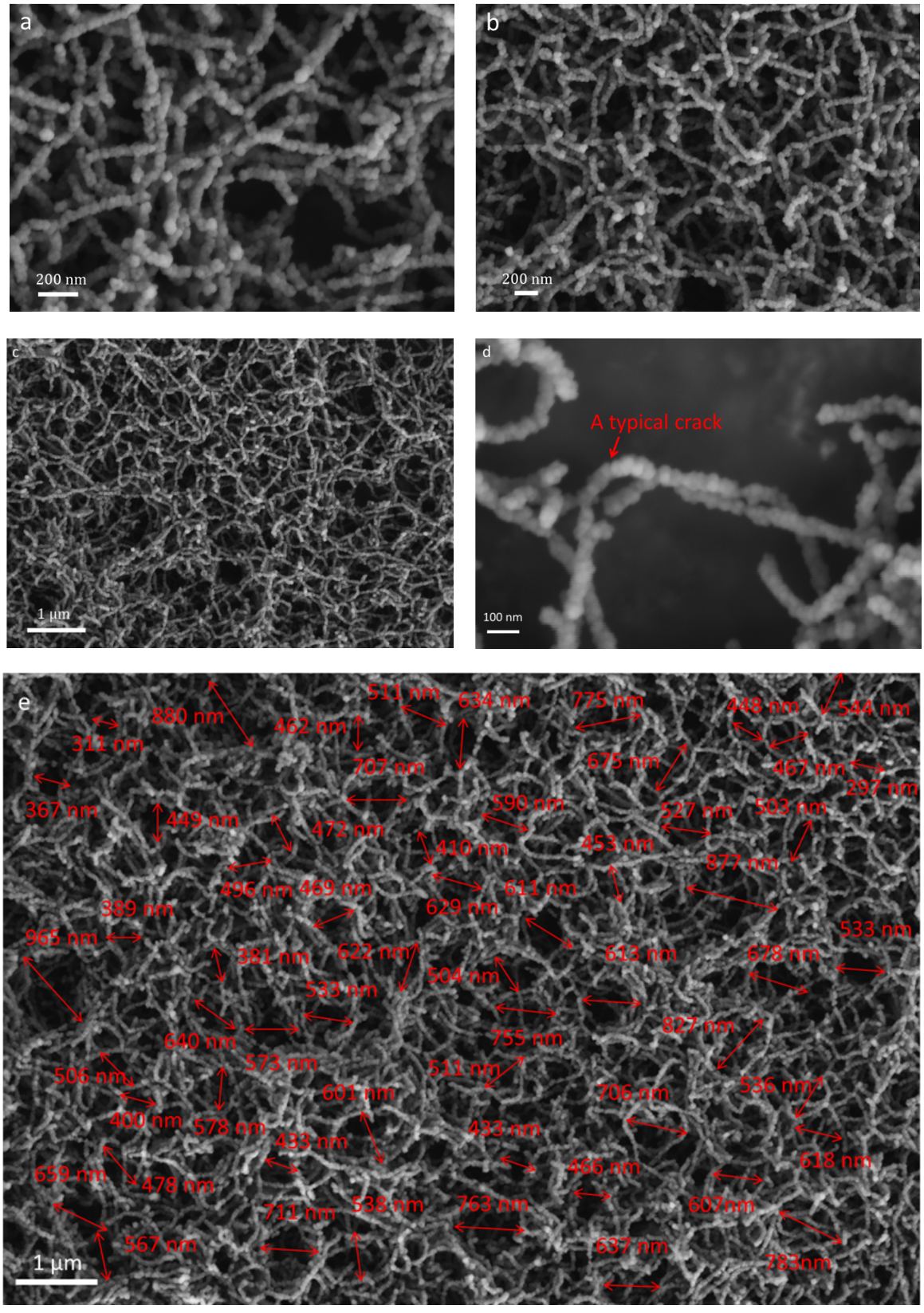
a
200 nm
b
200 nm
c
1 µm
d
A typical crack
100 nm
e
880 nm
311 nm
462 nm
511 nm
634 nm
775 nm
448 nm
544 nm
707 nm
675 nm
467 nm
297 nm
367 nm
590 nm
527 nm
503 nm
449 nm
472 nm
410 nm
453 nm
877 nm
496 nm
469 nm
611 nm
389 nm
629 nm
965 nm
533 nm
381 nm
622 nm
613 nm
678 nm
504 nm
533 nm
827 nm
640 nm
755 nm
573 nm
506 nm
511 nm
601 nm
706 nm
536 nm
400 nm
578 nm
433 nm
433 nm
659 nm
478 nm
466 nm
618 nm
711 nm
538 nm
763 nm
607nm
567 nm
637 nm
783nm
1 µm

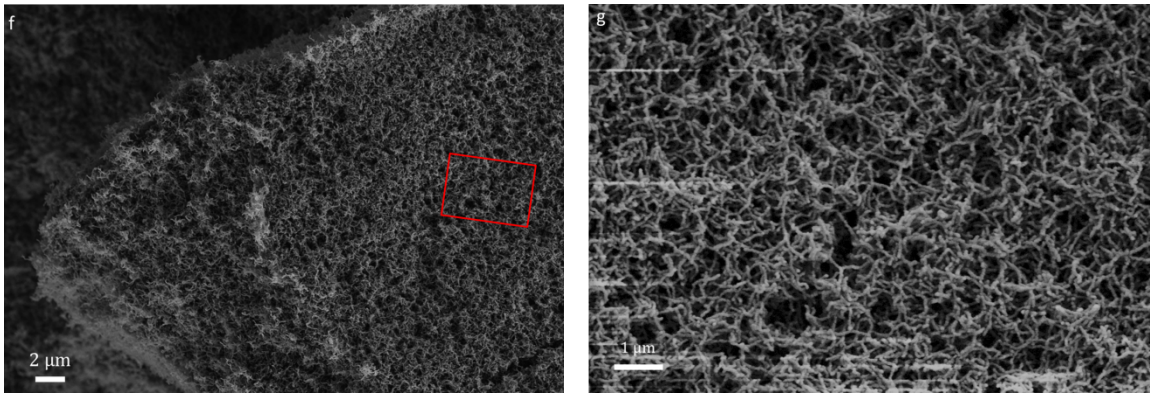

Figure S2. a-e) FESEM images of the 3D network, (e) shows that 3D network contains many macropores larger than 600 nm. f-g) FESEM images of Bulk-state 3D network after drying and activation, (f) is the magnification of the region showed by red square in (e).

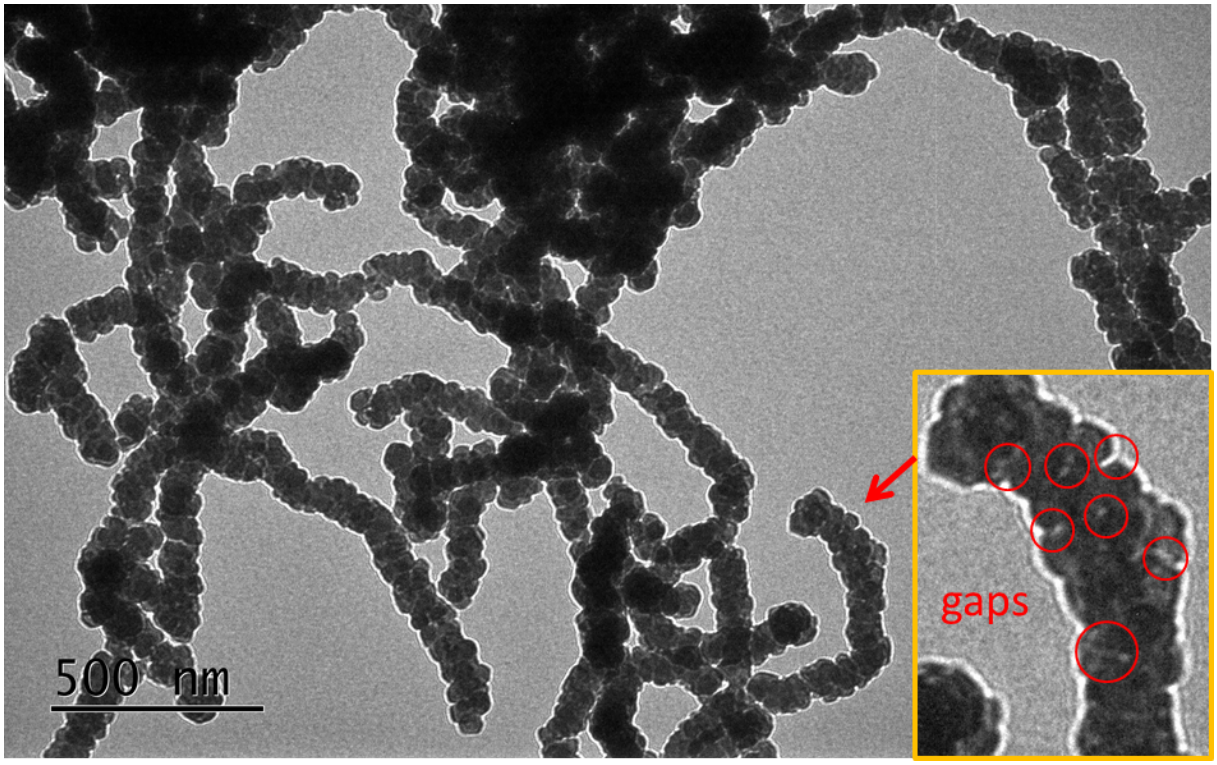

Figure S3. TEM image with large magnification of 3D networks, it indicates that the ZIF-8 layers of 3D networks were not smooth but full of mesopores derived from gaps between neighboring nanocrystals on ZIF-8 crystal layer (showed by the red circles).

S5: Mechanism of 3D network formation

1. Influence of PW's concentration

The concentration of PW plays an important role in formation of 3D networks with uniform width. When two times concentration of PW (0.16 mg/mL) was used, the 3D networks formed but the surfaces of PW were incompletely covered by the ZIF-8 (Figure S4a) and no free ZIF-8 nanocrystals formed in the solution was observed. Additionally, when one half concentration of PW (0.04 mg/mL) was used, the individual composite nanowires of which PWs were fully coated by ZIF-8 were formed. However, under this condition, homogeneous nucleation happened and many free ZIF-8 nanocrytals were formed in the solution (Figure S4c). The concentration of PW that we chose to fabricate 3D networks is in between these two concentrations (0.08 mg/mL) which guaranteed the formation of 3D networks and fully coverage of the PW at the same time (Figure S4b). Also, at this condition, there was no free ZIF-8 nanocrystal to be observed in the solution. These results also reveal that ZIF-8 prefers heterogeneous nucleation on the PW than in the solution.

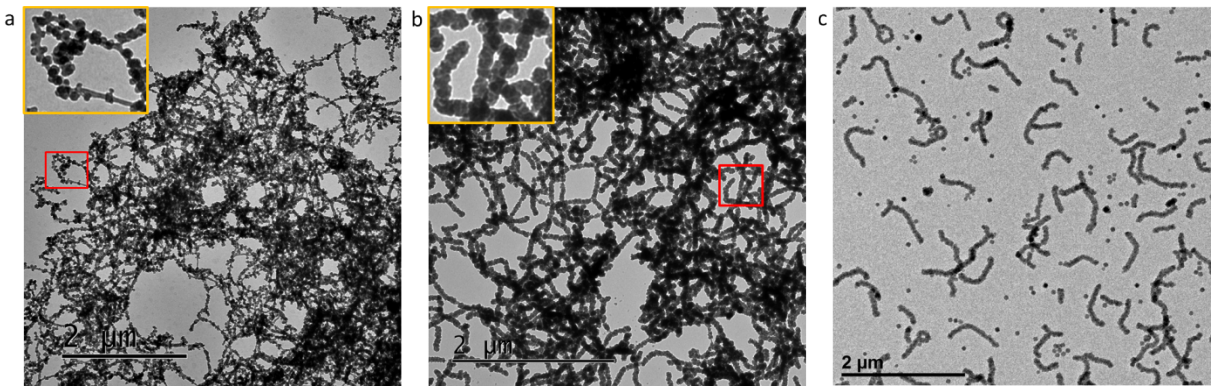

Figure S4. a-c) TEM images of composites formed by using different concentration of PW; a) 0.16 mg/mL, b) 3D networks: 0.08 mg/mL, c) individual composite nanowires: 0.04 mg/mL.

2. Influence of precursors' concentrations

The concentrations of precursors influence the crystal size of ZIF-8. When decreasing the concentrations of Zn2+ and 2-methylimidazole (Hmim) (Zn2+: 1.86 mg/mL, Hmim: 1.03 mg/mL), thin and non-uniform composite nanowires were produced (Figure S5a). And increasing the concentrations of Zn2+ and Hmim (Zn2+: 7.44 mg/mL, Hmim: 4.10 mg/mL and Zn2+: 11.16 mg/mL, Hmim: 6.15 mg/mL) resulted in larger size of ZIF-8 crystals coated on PW but incomplete coverage of PWs (showed by red arrows in Figure S5c-d). Therefore, the concentrations of precursors (Zn2+: 3.72 mg/mL and Hmim: 2.05 mg/mL) we chose to in the present study were the optimized concentrations to form 3D networks constructed from hybrid nanowires with a uniform width (Figure S5b).

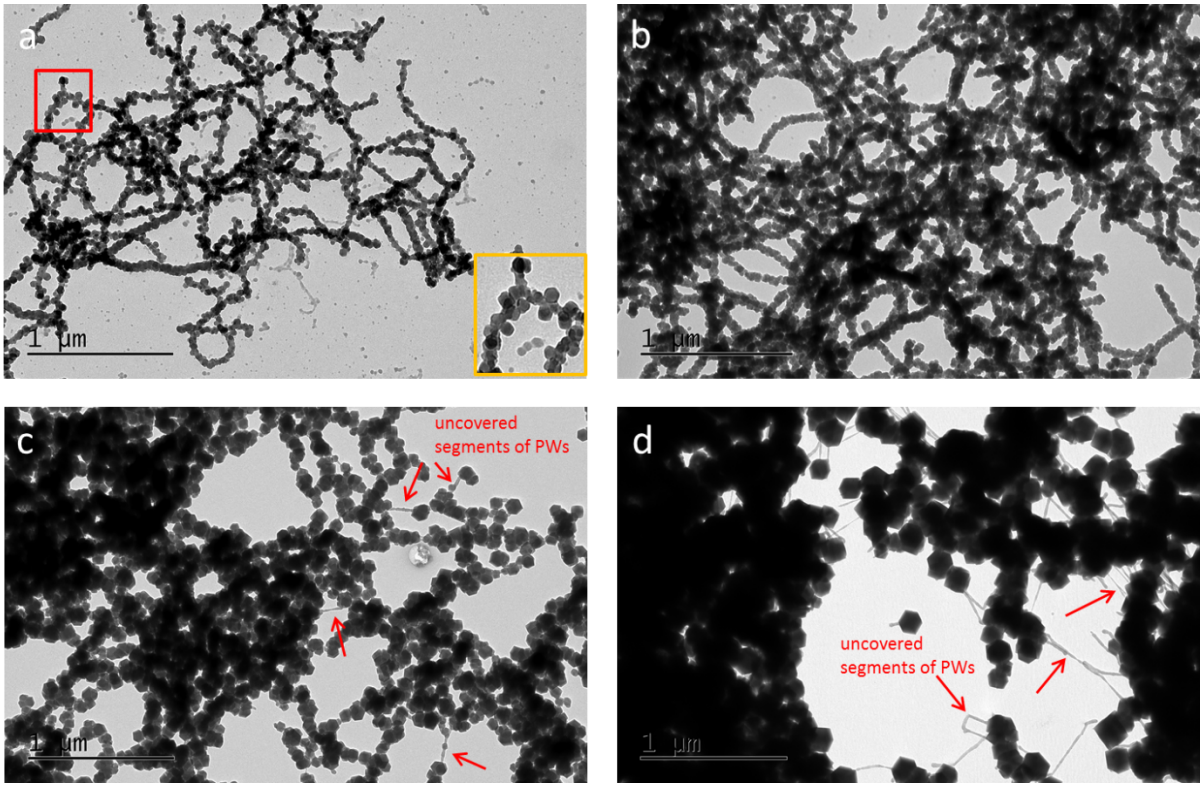

Figure S5. TEM images of composites formed by using different concentrations of precursors (the concentration of PWs is 0.08 mg/mL); a) Zn^{2+}: 1.86 mg/mL , Hmim: 1.03 mg/mL; b) 3D networks, Zn^{2+}: 3.72 mg/mL , Hmim: 2.05 mg/mL; c) Zn^{2+}: 7.44 mg/mL, Hmim: 4.10 mg/mL; d) Zn^{2+}: 11.16 mg/mL, Hmim: 6.15 mg/mL.

3. Control experiment: using highly crosslinked PWs as the template for preparing the composite nanowires

To direct the heterogeneous nucleation of ZIF-8, PWs need to interact with metal cations or ligands. The authors of previous studies have reported that, polymer polyvinylpyrrolidone (PVP) was incorporated into ZIF-8 through weak coordination interactions between oxygen atom of pyrrolidone rings (C=O) and Zn^{2+}.[2] In the present study, the TEM results indicated that the ZIF-8 layer mainly located in the shell of the PWs (Figure 1e). Therefore, we assumed that the interaction of the PEG shells (C-O-C) with Zn^{2+} primarily aided the heterogeneous

nucleation. This assumption is supported by the result of the control experiment that the100% crosslinked PWs can still direct the growth of ZIF-8 along the PW to form the composite nanowires (Figure S6).

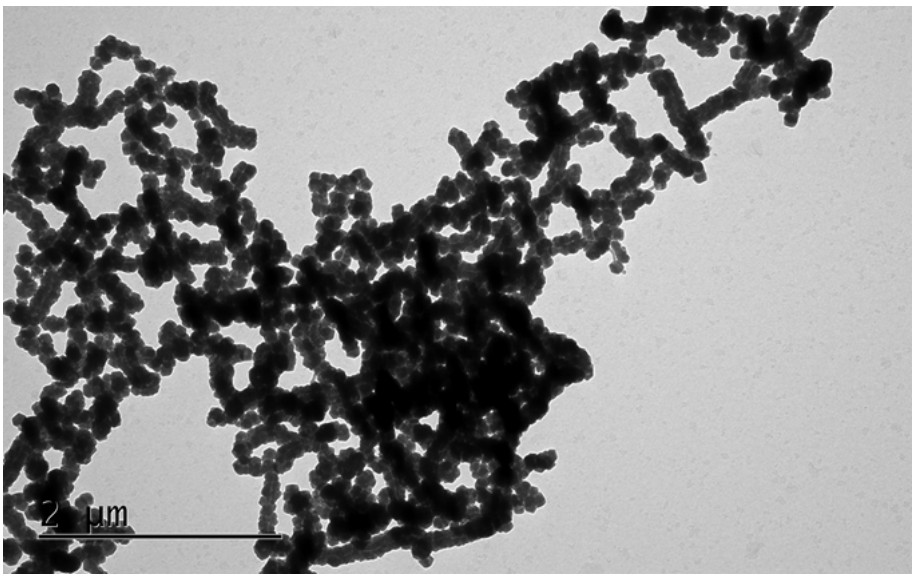

Figure S6. TEM images of highly crosslinked PWs-ZIF-8 composite nanowires.

4. Formation process traced by TEM

According to previous articles on the formation mechanisms of ZIF-8, the nucleation and growth of ZIF-8 in methanol at room temperature is rapid.[3] In the present study, crystal nucleation and growth on PWs were also very fast. In the beginning (< 5 min), spherical particles appeared on the PW and soon grew to cover the entire PW to form nanowires. Because of the high surface energy of the primary ZIF-8 nanoparticles, which are prone to fuse together when in contact with each other, the nanowires began to crosslink to each other. At 10 min, the nanowires became wider, and the networks became larger. At 1 h, the 3D networks had formed. The structure of 3D networks didn't change after 24 h incubation.

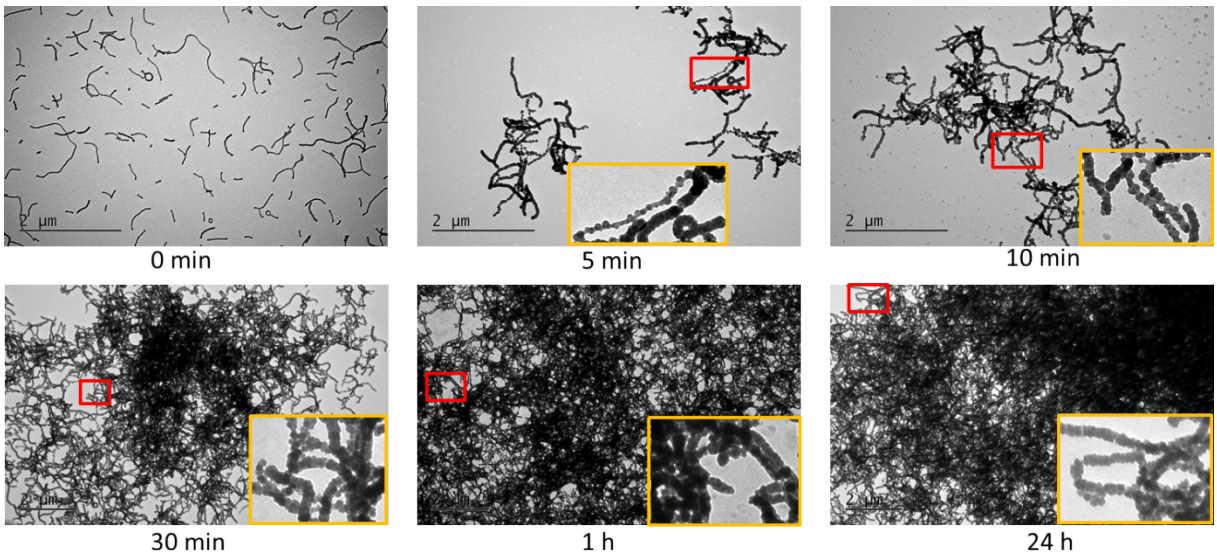

Figure S7. TEM images of the 3D networks as a function of synthesis time.

S6: Difference between 3D networks and individual composite nanowires

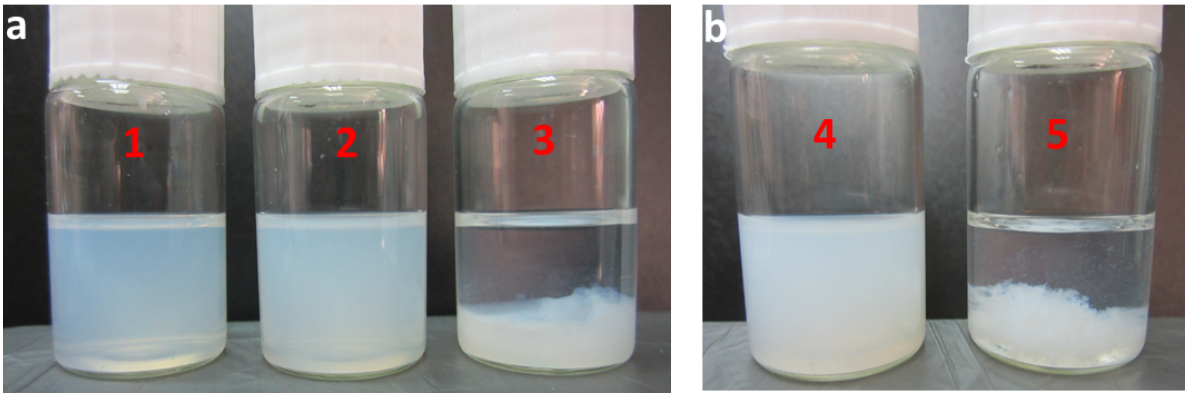

Figure S8. a) Reaction mixtures of pure ZIF-8 (nanocrystal) (1), individual composite nanowires (2) and the 3D network (3) (containing 0 mg/mL, 0.04 mg/mL and 0.08 mg/mL PWs respectively) after 24 h incubation. At PW concentration of 0.04 mg/mL, individual composite nanowires were obtained (see Figure S4c), which could be dispersed in methanol without precipitation (2). b) Individual composite nanowires (4) and 3D networks (5) redispersed in methanol at the same concentration. Individual composite nanowires could be re-dispersed in methanol without precipitation, whereas the 3D network maintained its floccule form.

Zeta potential of individual composite nanowires in methanol: +60mV (consistent with the sum of ZIF-8 (+48mV)[4] and 10% cross-linked PWs (+8.7mV)[1a])

S7: Pore-size distribution of micro- and mesopores

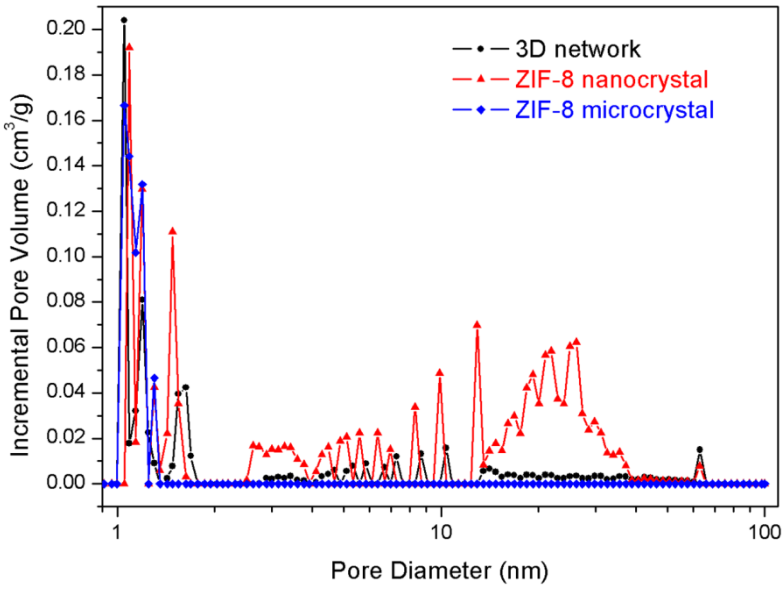

Figure S9. Pore-size distribution of micro- and mesopores calculated by NLDFT method based on the Nitrogen-sorption isotherms.

S8: Catalytic performance tests

Knoevenagel condensation, an important reaction generating C-C bond for synthesis of several fine chemicals,[5] is usually catalyzed by weak bases like primary, secondary, and tertiary amines under homogeneous condition. However, catalysts of homogeneous alkali are hard to be regenerated after reaction, and therefore, heterogeneous catalysts such as amino-functionalized mesoporous silica, zeolites exchanged with alkylammonium cations and MOFs were explored to catalyze Knoevenagel reaction.[6] MOFs were constructed through the assembly of metal ions and organic ligands. The metal ions (Lewis acid) and ligands (Lewis base) on the external surface of MOF particles are unsaturated and thus serve as the active sites. ZIF-8 is a prototypical MOF with a relatively high stability containing N- moieties which can serve as basic catalyst. Phan et al. reported that ZIF-8 was an efficient catalyst for Knoevenagel reaction at low temperature.[7] As the micropores of the ZIF-8 are as small as 3.4 Å, the large molecules could therefore not enter the micropores, and the catalytic reaction could only occur on the external surface of ZIF-8. Therefore, structuring ZIF-8 to improve its external surface and mass transport can improve the catalytic activity.

The Knoevenagel reaction of benzaldehyde with malononitrile was conducted in a 25 mL sample bottle with a magnetic stirring bar. In a typical reaction, a mixture of ZIF-8 catalyst (0.02 g), malononitrile (0.25 g, 3.8 mmol), and *n*-dodecane (0.2 mL) as an internal standard was added to a mixed solvent of 4 mL toluene and 1 mL THF. The solution was stirred to disperse the solid catalyst, and 0.2 mL of benzaldehyde (1.9 mmol) was subsequently added. The resulting mixture was stirred at 10 °C for 11 h. Reaction conversion was monitored by withdrawing

aliquots from the reaction mixture at different times and quenching with acetone. After being dehydrated using anhydrous $CaSO_4$, the samples were analyzed by GC.

Gas chromatographic (GC) analyses were performed on a HP6890 (PLUS) equipped with a flame ionization detector (FID) and a HP-INNOWax column (length = 30 m, inner diameter = 0.25 mm, and film thickness = 0.25 μm). The temperature program for GC analysis consisted of heating from 50 to 230 °C at 20 °C/min and then maintaining 230 °C for 3 min. The inlet and detector temperatures were set at 250 and 280 °C, respectively.

The selectivity of benzylidenemalononitrile is 90±2% calculated by the following formula: $Selectivity(\%) = n_p/n_r \times 100\%$. Where n_p and n_r represent the amount of benzylidenemalononitrile formed and benzaldehyde consumed, respectively.

S9: Pure nano- and micro-sized ZIF-8

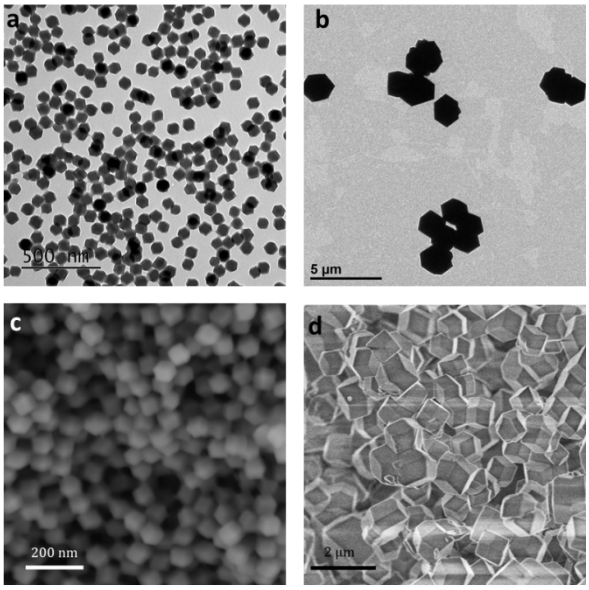

Figure S10. a-b) TEM images of pure ZIF-8 nanocrystals with diameters of approximately 65 nm and ZIF-8 microcrystals with diameters of approximately 1 μm. c-d) FESEM of bulk-state ZIF-8 nano- and micro-crystals.

1. (a) K. Zhang, M. Jiang and D. Chen, *Angewandte Chemie International Edition*, 2012, **51**, 8744-8747; (b) K. Zhang, J. Yi and D. Chen, *Journal of Materials Chemistry A*, 2013, **1**, 14649-14657; (c) K. Zhang, H. Miao and D. Chen, *Journal of the American Chemical Society*, 2014, **136**, 15933-15941.
2. G. Lu, S. Li, Z. Guo, O. K. Farha, B. G. Hauser, X. Qi, Y. Wang, X. Wang, S. Han, X. Liu, J. S. DuChene, H. Zhang, Q. Zhang, X. Chen, J. Ma, S. C. J. Loo, W. D. Wei, Y. Yang, J. T. Hupp and F. Huo, *Nat Chem*, 2012, **4**, 310-316.
3. (a) J. Cravillon, C. A. Schröder, R. Nayuk, J. Gummel, K. Huber and M. Wiebcke, *Angewandte Chemie International Edition*, 2011, **50**, 8067-8071; (b) J. Cravillon, S. Münzer, S.-J. Lohmeier, A. Feldhoff, K. Huber and M. Wiebcke, *Chemistry of Materials*, 2009, **21**, 1410-1412; (c) S. R. Venna, J. B. Jasinski and M. A. Carreon, *Journal of the American Chemical Society*, 2010, **132**, 18030-18033.
4. N. Yanai, M. Sindoro, J. Yan and S. Granick, *Journal of the American Chemical Society*, 2013, **135**, 34-37.
5. F. Freeman, *Chemical Reviews*, 1980, **80**, 329-350.
6. (a) K. M. Parida and D. Rath, *Journal of Molecular Catalysis A: Chemical*, 2009, **310**, 93-100; (b) C. F. Linares, M. R. Goldwasser, F. J. Machado, A. Rivera, G. Rodríguez-Fuentes and J. Barrault, *Microporous and Mesoporous Materials*, 2000, **41**, 69-77; (c) V. N. Panchenko, M. M. Matrosova, J. Jeon, J. W. Jun, M. N. Timofeeva and S. H. Jhung, *Journal of Catalysis*, 2014, **316**, 251-259.
7. U. P. N. Tran, K. K. A. Le and N. T. S. Phan, *ACS Catalysis*, 2011, **1**, 120-127.